Quantum Modeling of Nanoscale Symmetric Double-Gate InAlAs/InGaAs/InP HEMT

Neha Verma*, Mridula Gupta, R. S. Gupta***, and Jyotika Jogi***

***Abstract*—The aim of this work is to investigate and study the quantum effects in the modeling of nanoscale symmetric double-gate InAlAs/InGaAs/InP HEMT (High Electron Mobility Transistor). In order to do so, the carrier concentration in InGaAs channel at gate lengths (L_g) 100 nm and 50 nm, are modelled by a density gradient model or quantum moments model. The simulated results obtained from the quantum moments model are compared with the available experimental results to show the accuracy and also with a semi-classical model to show the need for quantum modeling. Quantum modeling shows major variation in electron concentration profiles and affects the device characteristics. The two triangular quantum wells predicted by the semi-classical model seem to vanish in the quantum model as bulk inversion takes place. The quantum effects thus become essential to incorporate in nanoscale heterostructure device modeling.**

***Index Terms*—Double-gate HEMT (DGHEMT), double triangular quantum well, modeling, quantum effects, simulation, symmetric**

Manuscript received Jul. 14, 2012; accepted May. 8, 2013
* Microelectronics Research Laboratory, Department of Electronic Science, A.R.S.D College, University of Delhi, South Campus, New Delhi 110021, India.
** Semiconductor Device Research Laboratory, Department of Electronic Science, University of Delhi, South Campus, New Delhi, India
*** Department of Electronics and Communication Engineering, Maharaja Agrasen Institute of Technology, New Delhi, India
E-mail : jogijyotika@rediffmail.com

I. INTRODUCTION

Novel device concepts are compelling for new sub-disciplines of microelectronics based on quantum structures. Importance of heterostructure consisting of ultrathin layers of semiconductors (quantum confinement devices) with their useful properties was introduced by Esaki and Tsu in 1970 [1]. In 1988 the low noise performance of InP-based HEMT surpassed that of GaAs-based PHEMT (Pseudomorphic HEMT) [2, 3]. Eventually InP-based InGaAs/InAlAs HEMT has emerged as one of the most promising high speed device [4-6]. Double heterojunctions and InAlAs/InGaAs DGHEMTs are widely accepted due to their larger 2-DEG (two-dimensional electron gas) concentration, better carrier confinement, greater current derivability and higher transconductance as compared to a single channel HEMT [7-10].

In order to improve the HEMTs performance, many attempts were made on scaling down its dimensions. As classical models evolved and showed a continuous improvement [11, 12] the role of quantum effects was largely ignored. It is worth emphasizing here that when carriers are restricted to regions with nanodimensions, their quantum energy levels begin to spread and quantum effects start appearing. As scaling down progressed from micro to nanodimensions, it became essential to understand the device as a quantum structure [13]. Nanodimensions led to an increased interest in modeling and predicting device performance prior to fabrication. Hence simulation of these devices including quantum effects was taken up for SGHEMT (single-gate HEMT) [14, 15]. To trace how the dominant trends of quantum effects are impacting DGHEMT, new challenges are

directed on the device simulator to identify the limiting and critical parameters for improved performance. This paper deals with the quantum effects in InAlAs/InGaAs/ InP double gate HEMT (DGHEMT) where the layers with confined electrons are so thin that the laws of quantum physics start manifesting themselves. The two 2-DEG layers formed in the channel between the two heterostructures cease to be independent and start behaving like a combined system. The authors in this work attempted to explore the effects due to quantum mechanical confinement in a channel formed by a double heterostructure device. The proposed quantum model treats the channel as a double triangular quantum well. The model used in this paper is quantum moments model or density gradient model. This model incorporates device characteristics like drain characteristics (I_D-V_{DS}), transfer-characteristics (I_D-V_{GS}), transconductance (g_m), output conductance (g_d), gate-source capacitance (C_{GS}), gate-drain capacitance (C_{GD}) and cut-off frequency (f_T) of InAlAs/InGaAs/InP DGHEMT. The results so obtained are compared with a semi-classical model (i.e. drift-diffusion mobility dependent model) and also with the available experimental data and are in good agreement.

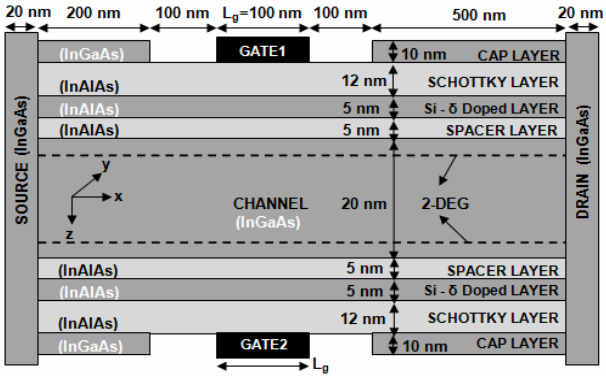

Fig. 1. Structure of simulated DGHEMT.

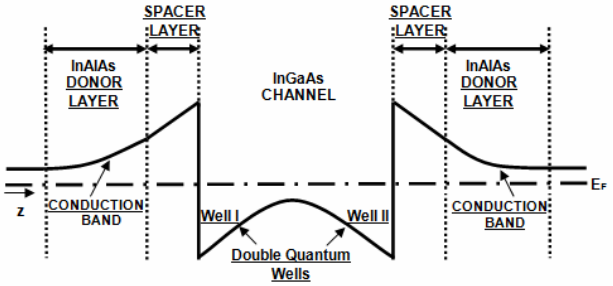

Fig. 2. Energy Band Diagram for a Double Heterostructure with Double Quantum Wells formed in z direction perpendicular to the channel.

II. METHOD

Quantization effects are revealed on considering the structure of DGHEMT which is designed as a double heterostructure device including two InAlAs donor layers characterized by their wider bandgaps and the central InGaAs layer as the channel with narrower bandgap. The schematic of the device is shown in Fig. 1. The source and drain contacts are modelled as areas with high values of doping. The source, drain and gate are defined as electrodes in the simulation program. Also, in ATLAS device simulator [16], an electrode in contact with semiconductor material is assumed by default to be ohmic which are source and drain and for a schottky contact (for GATE 1 and GATE 2), a workfunction has to be defined in CONTACT statement which are defined in the simulation program as 4.69 eV. Also, the electron mobility is defined as 8300 cm^2/V-s and the saturation velocity as $2.63x10^7$ cm/s.

The carriers are presumed to be confined inside the two quantum wells formed due to the electron band discontinuities and the difference in electrostatic field of electrons or remote ionized impurities near the hetero-junction. The energy-band diagram of a double heterostructure is shown in Fig. 2. Quantum modeling of nanoscale heterostructures requires the carriers to be treated as waves with their wave functions changing continuously. Consequently, the density in the quantum well does not peak abruptly but changes gradually. Hence the charge carrier distribution function needs to be modified. Because of the wave function extension into the barriers, which may further extend into the second quantum well, the carrier does not always confine itself to the minimum potential in one quantum well but are also experiencing the variable neighbouring potentials. This continuous change in the wavefunction and the consequent deviation of the carrier concentration profile from classical approach requires a quantum correction term to be included in the modeling.

In order to accurately profile the carrier concentration in the channel, the quantum moments (density gradient) model has been used to simulate the channel confinement in nanoscale DGHEMT [16]. The density gradient is a

continuum approach and is a fully self-consistent treatment of the problem. Density gradient theory was developed to account for quantum effects specifying the equation of state of electron gas which is energetically sensitive not only to its density but also to the density gradient. It can also be observed as a modification of normal drift-diffusion model.

The density gradient model is derived as a moment expansion of the Wigner-Boltzmann or a corresponding Quantum Liouville equation [17]. Classically the moments of the Boltzmann equation are taken with respect to momentum which attains a simpler form of equations, but it becomes impractically complex for the quantum mechanical applications. Therefore in order to reach at much simpler equations for the quantum part which should be comparable to the classical simplicity, the method of moments is applied to the Wigner equation. This leads to equations that contain additional quantum correction terms. In the quantum drift-diffusion method, a high order moment appears in each of the moment equation and by making an approximation for the highest moment, the hierarchy can be truncated at some point [18].

The moment equation hierarchy can be closed on a level corresponding to the drift-diffusion equation by omitting the time derivatives and the convective terms quadratic in $\vec{J}$ and consequently the current equation (in lowest order Born approximation) can therefore be given by [19]:

$$e\vec{J} = -\mu k_B T \nabla n - \mu n \nabla \Phi - \mu \left(\nabla \frac{\hbar^2 n}{4 m^* k_B T} . \nabla \right) \nabla \Phi_q \quad (1)$$

where e is the elementary charge, μ is the field dependent mobility, k_B is the Boltzmann constant, T is the temperature in absolute, m^* is the effective mass and n is the particle density given by:

$$n \propto \exp\left[\beta\left(E_F - \Phi\right)\right] \quad (2)$$

where E_F represents quasi-Fermi potential and $\beta = \frac{1}{k_B T}$ is the reciprocal carrier thermal energy.

$\Phi = q\phi + \Phi_B$; is the potential (consisting of both an electrostatic part φ with q as particle charge and band edge contribution Φ_B) and the quantum correction Φ_q is incorporated as [19]:

$$\Phi_q\left[\vec{R}\right] = \left(\frac{2m^*}{\pi\hbar^2\beta}\right)^{d/2} \int d^d R' \Phi\left[\vec{R}' + \vec{R}\right] I_d\left[\frac{2m^* R'^2}{\hbar^2\beta}\right] \quad (3)$$

here d is the dimensionality (degrees of freedom) of the physical system (mesh) and $\vec{R} = \frac{\vec{x} + \vec{y}}{2}$; is 3D (centre of mass) position coordinate with $\vec{x}$ and $\vec{y}$ coordinates. Since Eq. (3) is numerically complex to solve in the device simulation. For this we take $l_{qm} = \sqrt{\frac{\hbar^2\beta}{2m^*}}$ as the characteristic quantum length scale and assume a slow variation of potential Φ on this length scale of l_{qm} [17]. This simplifies Eq. (3) to $\Phi_q = \Phi / 3$.

Under equilibrium we can assume:

$$\log n = \beta(E_F - \Phi) + O(\hbar^2) + const.; \quad (4)$$

So that the last term in Eq. (1) becomes:

$$\left(\nabla \frac{\hbar^2 n}{4 m^* k_B T} . \nabla \right) \nabla \Phi_q = \frac{\hbar^2 \beta n}{12 m^*} \left(\nabla \nabla^2 \left(E_F - \Phi\right) - \beta \left[\left(E_F - \nabla\Phi\right) + \left(\nabla O\left[\hbar^2\right] \right) \right] \nabla \left(E_F - \nabla\Phi\right) \right) \quad (5)$$

In the above equation, the term $O[\hbar^2]$ can be omitted in lowest order quantum correction as it gives a negligible contribution of the order of $\hbar^4$ which is below the accuracy where the quantum correction potential Λ is given by:

$$\Lambda = \frac{\hbar^2\beta}{12 m^*} \left[\nabla^2 (E_F - \Phi) - \frac{\beta}{2} \left(E_F - \nabla\Phi\right)^2 \right] \quad (6)$$

This alters the Eq. (1) to the following form:

$$e\vec{J} = -\mu k_B T \nabla n - \mu n \nabla \left(\Phi + \Lambda\right) \quad (7)$$

But still Φ is discontinuous at material interfaces and might have abrupt jumps, so Λ in Eq. (6) might remain

undefined at some points. Hence a fitting parameter γ is introduced in Eq. (6) to slightly modify Λ as:

$$\Lambda = \frac{\gamma\hbar^2\beta}{12m^*}\left[\nabla^2(E_F-(\Phi+\Lambda))-\frac{\beta}{2}\left(E_F-(\nabla\Phi+\nabla\Lambda)\right)^2\right] \tag{8}$$

The explanation for doing so is the dilemma about which value to use for the effective mass for a semiconductor with multiple conduction band minima. Thus we introduce fitting parameter γ and take m as the density of states mass.

Further Eq. (8) is modified by adding $\Phi_m = -\frac{d}{2}k_BT\log m$ to the potential Φ in the right hand side [19], so that the equation becomes:

$$\Lambda = \frac{\gamma\hbar^2\beta}{12m}[\nabla^2(E_F-(\Phi+\Phi_m+\Lambda))- \frac{\beta}{2}(E_F-(\nabla\Phi+\nabla\Phi_m+\nabla\Lambda))^2] \tag{9}$$

Thus the particle density with the quantum correction potential is given by:

$$n \propto \exp\left[\beta\left(E_F-(\Phi+\Phi_m+\Lambda)\right)\right] \tag{10}$$

Following Eq. (10), for the correct charge distributions in the channel, Eq. (9) can also be written as:

$$\Lambda = -\frac{\gamma\hbar^2}{12m}\left[\nabla^2\log n+\frac{1}{2}\left(\nabla\log n\right)^2\right] = -\frac{\gamma\hbar^2}{6m}\frac{\nabla^2\sqrt{n}}{\sqrt{n}} \tag{11}$$

The quantum corrected expression for the current density $\vec{J}$ is given by:

$$\vec{J} = -\mu k_BT\nabla n-\mu n\nabla(\Phi+\Phi_m+\Lambda) \tag{12}$$

Together with the Poisson's equation

$$div\left(\varepsilon\nabla\phi\right) = -\rho\,; \tag{13}$$

ε is the permittivity and ρ is the space charge density and continuity equation (Eq. (14)) with Eq. (11) together forms a system that have to be solved self-consistently [20].

$$\frac{\partial n}{\partial t} = \frac{1}{q}div\vec{J}+G-R\,; \tag{14}$$

G and R are generation and recombination rates for carriers. The above set of equations outlines the formulation of density gradient model and is incorporated in the simulation. The quantum effects are studied at gate lengths 100 nm and 50 nm. Small values of L_g invoke short-channel effects which limit the microwave performance of the HEMTs because the gate capacitance does not continue to scale with the gate length for such small values of L_g, so to avoid these effects, a vertical scaling of the layer structure must go along with the reduction of the gate length in order to keep a high aspect ratio. In both the simulated DGHEMT structures, the aspect ratio is effectively higher i.e. ≈ 4.5 and ≈ 2.27 for 100 nm and 50 nm DGHEMT respectively. The respective device dimensions for L_g=100 nm and 50 nm are given in Table 1. Also, in the simulated structure, delta doping plane is modeled as 5 nm InAlAs layer with doping level of $5x10^{12}$ cm^{-2} which gives a doping range of 10^{19} cm^{-3} or 10^{25} m^{-3}. Thus, the donor concentration of the delta doped layer is incorporated as $2.8x10^{18}$ cm^{-3} or $0.28x10^{19}$ cm^{-3} from the available doping range so as to obtain the threshold voltage as it is given for the device in experimental results [21].

Table 1. Device Dimensions

Device Dimensions		
Layer	Doping	Dimensions (Thickness) nm
Cap ($In_{0.53}Ga_{0.47}As$)	$6*10^{18}$ cm^{-3}	10
Undoped Schottky ($In_{0.52}Al_{0.48}As$)	(non-intentionally-doped) nid	12
δ-doped Layer ($In_{0.52}Al_{0.48}As$)	$2.8*10^{18}$ cm^{-3}	5
Spacer ($In_{0.52}Al_{0.48}As$)	nid	5
Channel ($In_{0.53}Ga_{0.47}As$)	nid	20

2.1 Model Implementation

Many analytical and numerical methods have been developed for describing the device characteristics. Among the semi-classical models, Monte Carlo model offers the detailed explanation of solution but is limited in realistic engineering applications for its computational expenses [22]. On the other hand, drift-diffusion equations are advantageous as they are the most general and commonly used set of equations in hetero-junction device simulation codes. Thus, the authors have used quantum moments model which is also known as quantum drift-diffusion method (density-gradient model) and compared it with a semi-classical drift-diffusion model. This has helped in observing the change from drift-diffusion modeling to quantum drift-diffusion modeling (where the quantum confinement is included). Quantum moments model is a proficient model to describe various effects of quantum mechanical confinement. It maintains the explicit quantum corrections as well as the features of the classical hydrodynamic model and is also compatible with the drift-diffusion treatment used in device simulator. Carrier distribution near interfaces which are not accurately described by the semi-classical models can be accurately reproduced by the quantum moments model.

Both the semi-classical and quantum models are implemented using ATLAS device simulator version 5.16.3.R. The semi-classical or drift-diffusion model comprises of three basic equations i.e. a poisson's equation which relates the local charge density and the electric field and two continuity equations ensuring the charge conservation of the device. In this method, current density is expressed in terms of the quasi-Fermi level which is then linked to the carrier concentration and the potential through the Boltzmann approximations. Equations are re-written to define the quasi-Fermi potential and finally substituting them into the current density expressions allowing the form of equations used in simulation program for current. On the other hand, quantum moments model is derived as a moment expansion of the Wigner-Boltzmann equation which is already described above in detail. The carrier distribution given by the density gradient model can change greatly from the distributions predicted by the standard drift-diffusion model [16]. Therefore, the initial guess methods are not suitable enough for the quantum moments model. Hence, a damping factor is applied gradually, specified by the QFACTOR (value between 0.0 and 1.0) [16] which is implemented as a pre-factor to the expression of the quantum correction potential to overcome the convergence problems (convergence problems increase the run-time of the program) to obtain the electron concentration and consequently the other parameters of the device. However, limitations of the quantum moments model include a fine meshing according to the optimization of the structure (with the scaling of the gate length) to improve the run-time of the simulation program and cannot predict bound state energies or wave functions.

III. Results and Discussion

Fig. 3(a) and (b) show the electron concentration profiles using both quantum moments model (density gradient model) and semi-classical model (drift-diffusion model) at gate lengths (L_g) 100 nm and 50 nm, respectively. The most prominent difference between the semi-classical model and quantum model is in the distribution of the carriers. In the semi-classical case the electron concentration is seen to peak towards the two channel interfaces in the heterostructure, while for the quantum mechanical solution, the peak of the electron concentration is located in the middle of the channel for the same bias conditions, clearly indicating the effect of quantum modeling. The two quantum wells predicted by semi-classical model seem to vanish in the quantum moments model at nanodimensions thus resulting in a distribution of carriers along the entire depth of the channel. As the channel and consequently the boundary between the wells are reduced to nanodimensions, there will be an expected tunnelling from the two wells into the barrier. This redistribution in addition to being dependent on the channel dimensions will also be greatly affected by the transverse electric field applied along the z direction. Thus the two gate potentials will play a major role in the re-distribution of charge carriers along the depth of the channel. Thus the finite probability of an electron penetrating into the barrier [23] or from one well to the other is one of the most important manifestations of quantum modeling approach for the DGHEMT. This could lead to a physical phenomenon that can be exploited

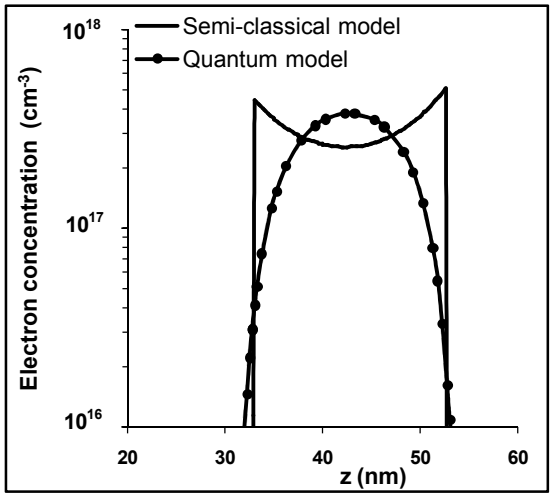

Fig. 3(a). Electron concentration profile under the gate for 100 nm DGHEMT. V_{DS}=0.5 V and V_{GS} =-0.1 V.

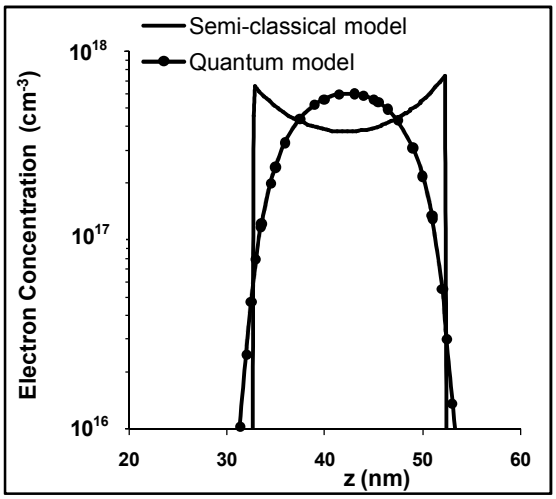

Fig. 3(b). Electron concentration profile under the gate for 50 nm DGHEMT. V_{DS}=0.5 V and V_{GS}=-0.1 V.

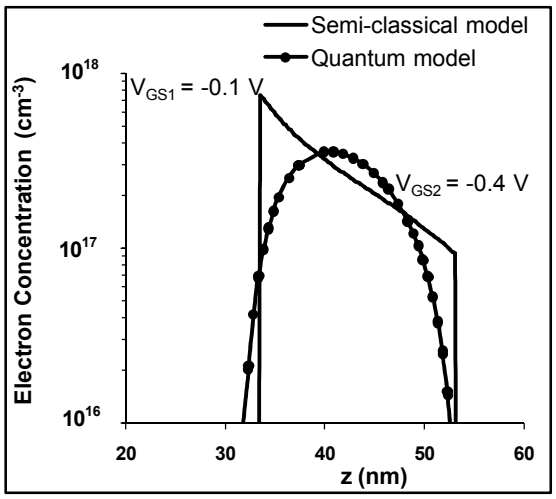

Fig. 3(c). Electron concentration profile under the gate for the 50 nm DGHEMT, V_{DS} =0.5 V.

for future application. This tunnelling provides coupling between two quantum wells whose spectrum then seems to behave as that of a single quantum well.

The maximum electron concentration obtained using the quantum approach is found to be 6×10^{17} cm^{-3} and 3.77×10^{17} cm^{-3} for 50 nm and 100 nm DGHEMT respectively. It is observed that the peak value of the electron concentration for 50 nm DGHEMT is almost one and half times higher in comparison to 100 nm DGHEMT, thus establishing a possibility of a higher current.

Fig. 3(c) shows the effect of different gate voltages applied on the two gates placed at the top and the bottom of the DGHEMT as shown in Fig. 1. The electron concentration profile shown here is obtained at V_{GS1}=-0.1 V, V_{GS2}=-0.4 V and V_{DS}=0.5 V for 50 nm DGHEMT. As seen here, the carriers start depleting from the interface closer to the more negative gate i.e. GATE2 and move towards the interface closer to the less negative gate i.e. GATE1. As a result, the peak of the electron concentration shifts towards the GATE1 which is at a higher voltage as compared to GATE2.

The simulated I_D-V_{DS} characteristics for both quantum and semi-classical model are plotted and are also compared with the experimental results [21] for 100 nm DGHEMT at V_{GS}=-0.1 V and -0.2 V in Fig. 4. It can be seen that the quantum model has a better matching with the experimental results [21] as compared to the semi-classical model. Thus validating the importance of following a quantum model for nanoscale DGHEMT. Further, the current between the source and drain is controlled by applying a voltage to the gate. This applied gate voltage alters the carrier density and consequently the current through the channel formed by the two triangular quantum wells in the InGaAs layer near the hetero-interface and this change of current can be clearly observed in the figure at two different gate voltages i.e. V_{GS}=-0.1 V and -0.2 V.

Fig. 5 presents the comparison of 100 nm and 50 nm simulated quantum results for V_{GS} values varying from 0 to -0.2 V with a 0.1 V step. The reduction in the gate length from 100 nm to 50 nm shows an increase in the current level which is attributed to the higher carrier concentration in 50 nm DGHEMT due to better carrier confinement in terms of a higher peak for carriers in the channel as compared to a 100 nm DGHEMT. But, the

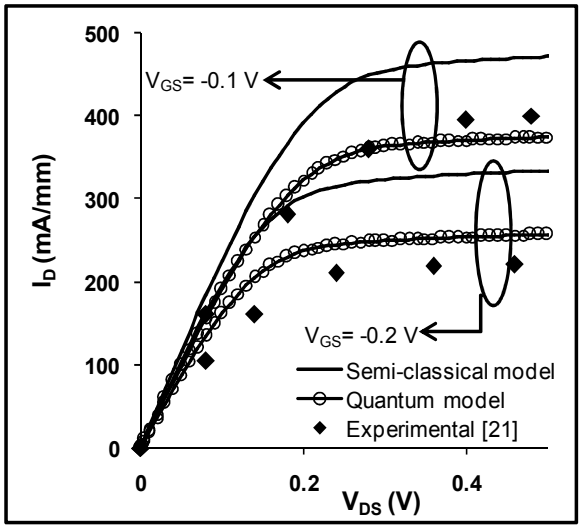

Fig. 4. I_D–V_{DS} characteristics for 100 nm DGHEMT.

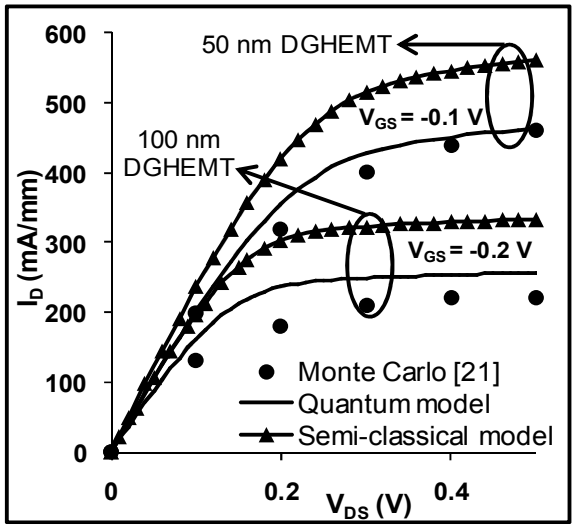

Fig. 6. I_D–V_{DS} characteristics for 50 nm and 100 nm DGHEMT compared with the simulated results of [21].

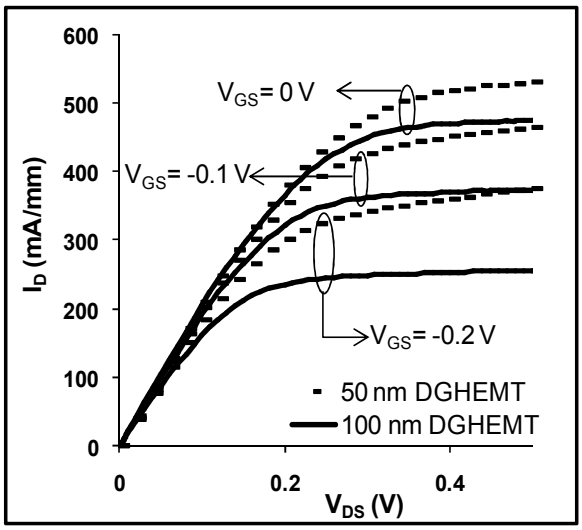

Fig. 5. I_D–V_{DS} characteristics of 100 nm and 50 nm DGHEMT for quantum model.

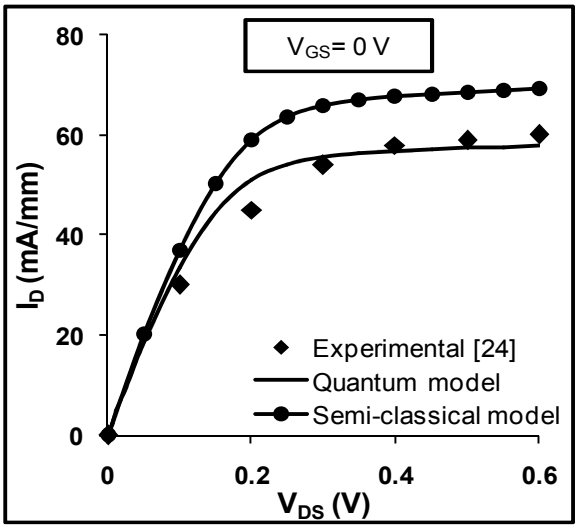

Fig. 7. I_D–V_{DS} characteristics for a long channel DGHEMT.

current in 50 nm DGHEMT does not increase by the same factor as it does for the electron concentration because the 2-DEG formed at the two hetero-junctions behaving like a double quantum well (DQW) are not independent now, instead they merge to behave like a single quantum well (SQW) as there will be an expected tunnelling from the two wells into the barrier due to which the corresponding drain current also reduces.

In order to investigate the limitation of the quantum model used with gate length, the authors have compared the quantum results with the simulated results of [21] for both 100 nm and 50 nm. Fig. 6 presents the I_D-V_{DS} characteristics for 50 nm and 100 nm DGHEMT at V_{GS} = -0.1 V and -0.2 V respectively. The quantum moments model used in the paper seems to have no limitation upto scaling down to 50 nm gate length as seen in Fig. 6. The authors did not use Monte Carlo model due to its limitations already mentioned in the previous 2.1 section.

Fig. 7 presents simulated quantum and semi-classical results compared with the experimental results of a long channel double gate HEMT (gate lengths for bottom and top gates are 1.2 μm and 1.4 μm respectively) [24]. The structure of the simulated long channel DGHEMT is shown in Fig. 8 which displays all the device dimensions, material used and the necessary parameters like doping concentration of each layer. However, the workfunction

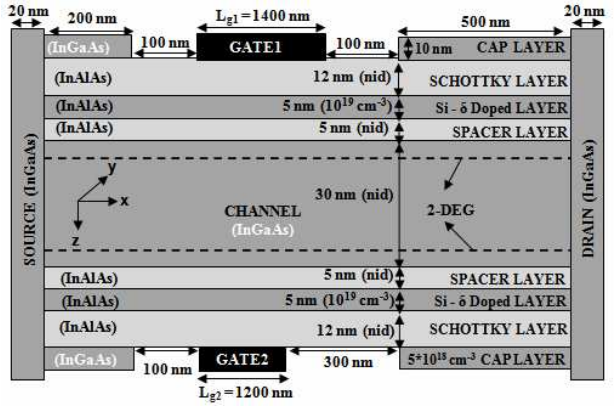

Fig. 8. Simulated structure of long $In_{0.52}Al_{0.48}As$/ $In_{0.53}Ga_{0.47}As$ DGHEMT with different gate lengths.

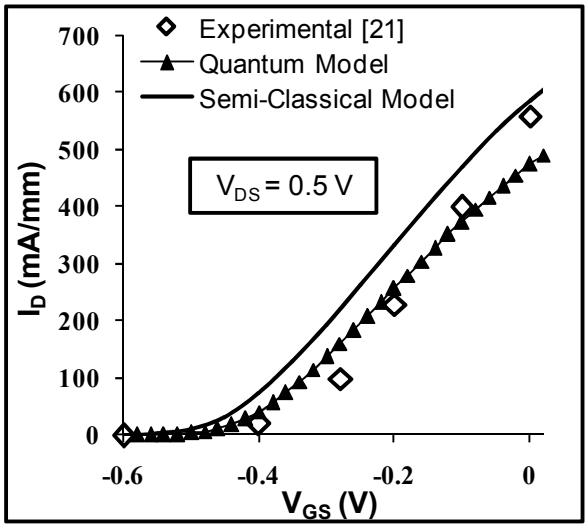

Fig. 9. I_D–V_{GS} characteristics for 100 nm DGHEMT for V_{DS} = 0.5 V.

for the schottky contact (for GATE 1 and GATE 2) is 4.69 eV, electron mobility as 8300 cm^2/V-s and the saturation velocity is defined as $2.63x10^7$ cm/s in the simulation program.

Fig. 7 demonstrates I_D-V_{DS} characteristics for V_{GS} = 0 V. The graph explains the importance of the proposed quantum model in a long double-gate nanoscale hetero-structure device. Here, a quantum model is applied for modeling a DGHEMT with channel thickness 30 nm and two long gates on the top and the bottom of the two identical heterostructures [24]. Quantum model shows a better match with the experimental results as it models the quantum effects prevailing in the channel where the two quantum wells are interacting due to its nano-dimensions. The figure demonstrates the importance of quantum modeling in long double-gate nanoscale hetero-structures but for the enhanced performance of the device, short channel devices are preferred as it reduces the transit time of the electrons that they have to travel making the device faster. Hence, this paper concentrates on 100 nm and 50 nm DGHEMT device only.

Fig. 9. shows the drain current dependence on gate-source voltage for 100 nm DGHEMT at constant V_{DS}, where the simulated quantum and semi-classical models are compared with available experimental results [21]. The quantum moments model is in better agreement with the available experimental results as compared to semi-classical model. Also, the quantum model shows better matching with the available experimental results in low voltage region in comparison to high voltages. This is because the 2-DEG formed at the two hetero-junctions behave like a double quantum well (DQW) in the field of operation corresponding to positive voltages. These DQW merge to behave like a single quantum well (SQW) as the gate bias is made negative. Hence, the quantum model which incorporates this effect treats the DQW as an equivalent SQW even for the positive voltages and thus the mismatch at positive voltages. But, in the region of operation of DGHEMT, quantum model gives a good match with the experimental already shown in Fig. 7.

The transconductance is considered to be one of the important parameter of the device as it decides the ultimate speed of a switching device along with some interconnect capacitances. The larger the transconductance greater is the gain and higher is the speed, which makes it the most important indicator for high-frequency applications. Fig. 10 shows the transconductance (g_m) for 100 nm and 50 nm DGHEMT at fixed drain-to-source voltage V_{DS} = 0.5 V.

The transconductance of 100 nm DGHEMT using present quantum model is 1209 mS/mm and 1000 mS/mm of 50 nm DGHEMT. As can be seen, that these values of transconductance are lower in comparison to those obtained using semi-classical approach for both the 100 nm and 50 nm DGHEMTs. In addition, the device transconductance is greatly affected by device dimensions and channel material properties. Also, when there is a decrease in the gate length, an increase of transconductance would be presumed, but this does not happen here as the figure shows that the 100 nm gate length has better

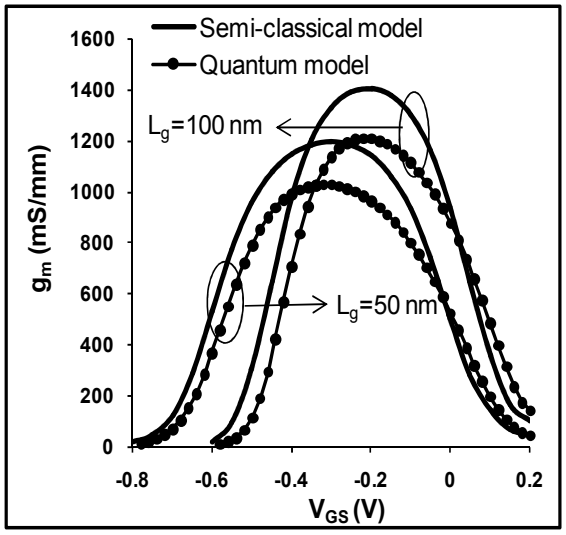

Fig. 10. g_m versus V_{GS} for 50 nm and 100 nm DGHEMT, V_{DS} = 0.5 V.

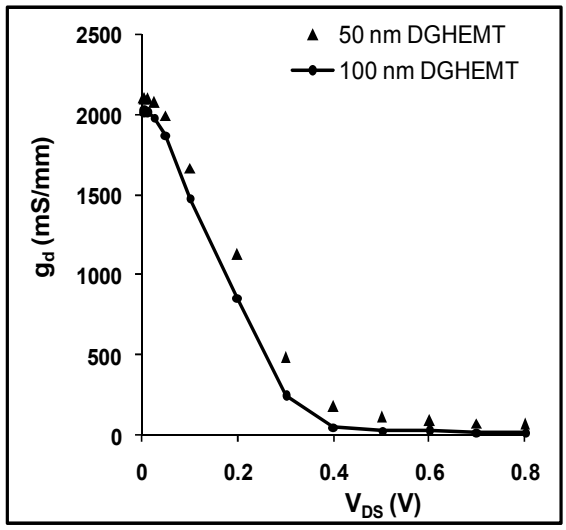

Fig. 11. g_d versus V_{DS} for 100 nm and 50 nm DGHEMT, V_{GS} = -0.1 V.

transconductance than 50 nm. This is because of the non optimized layer structure of 50 nm gate length device [21]. It has been reported [25] that InGaAs HEMTs perform well for aspect ratio value 7.5 and 4-5 for negligible and reduced short-channel effects and as defined above, the aspect ratio for 50 nm DGHEMT is below 4 (i.e. (L_g/a = 2.27 < 4)) and therefore suffers from short channel effects. The authors used the experimental results from [21] for comparison and hence simulated the same structure that had been fabricated for 100 nm by scaling the gate length to 50 nm.

The output conductance (g_d), which is defined as the ratio of incremental change in the drain current due to an incremental change in the drain-to-source voltage at fixed gate-to-source voltage is plotted in Fig. 11 for both 100 nm and 50 nm DGHEMTs. Output conductance plays an important role in determining the maximum voltage gain attainable from the device. A slight increase is observed in 50 nm DGHEMT as compared to 100 nm as the output conductance tends to increase with a reduction in gate length.

C_{GS} and C_{GD}, gate-source and gate-drain capacitances model the change in the depletion charge with respect to the gate-source and gate-drain voltages and directly affect the frequency response of the device. Fig. 12 shows the variation of C_{GS} with V_{GS} for the 100 nm and 50 nm DGHEMT at a fixed V_{DS} = 0.5 V comparing semi-classical and quantum results. The reduction in the gate length affects the capacitances as the value of C_{GS} is

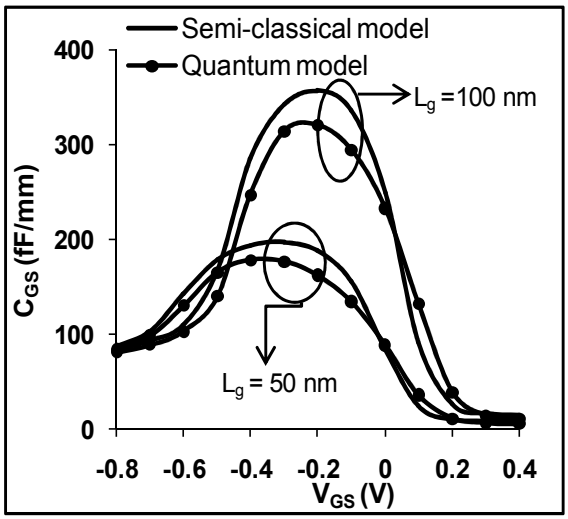

Fig. 12. C_{GS} versus V_{GS} for 100 nm and 50 nm DGHEMT, V_{DS} = 0.5 V.

lower for the 50 nm DGHEMT as compared to the 100 nm. Fig. 13 shows the variation of C_{GD} with V_{GS} for the 100 nm and 50 nm DGHEMT obtained using both quantum moments model and semi-classical model. The gate-drain capacitance is seen to be same at negative gate voltages, for both the models.

Finally the cut off frequency of the device is investigated in Fig. 14. for both the gate lengths using both quantum and semi-classical models. The cut off frequency is plotted as a function of V_{GS} at V_{DS} = 0.1 V and 0.5 V (inset). As expected, f_T increases strongly with decrease in L_g. This is because the transit time of the electrons decreases across the channel with the reduction

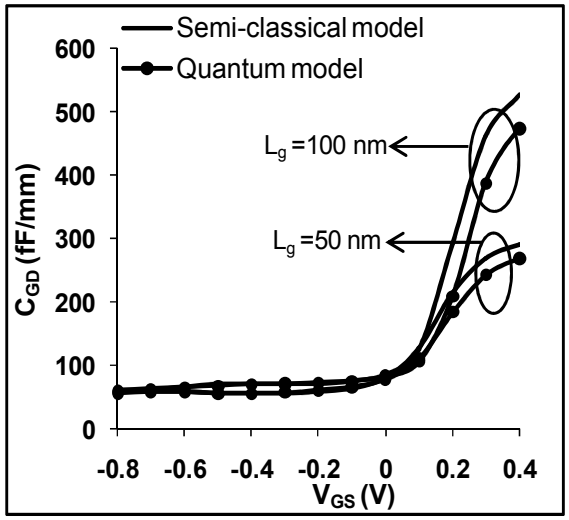

Fig. 13. C_{GD} versus V_{GS} for 100 nm and 50 nm DGHEMT, V_{DS} = 0.5 V.

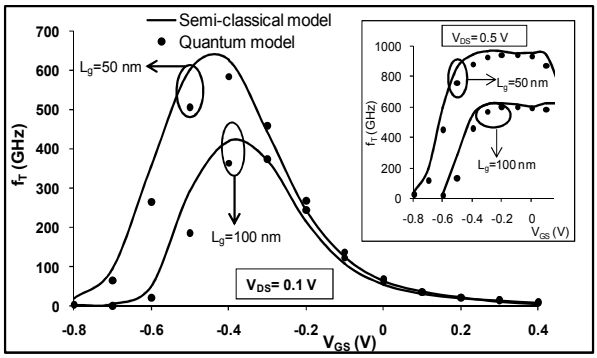

Fig. 14. f_T versus V_{GS} for 100 nm and 50 nm DGHEMT at V_{DS} = 0.1 V and 0.5 V (inset).

in the gate length. Also an increase of g_m in 100 nm DG-HEMT with respect to 50 nm DGHEMT is compensated by the higher values of C_{GS}, therefore providing higher values of cut- off frequency f_T for 50 nm DGHEMT as compared to 100 nm DGHEMT.

IV. CONCLUSIONS

Quantum moments model has been applied to nanoscale symmetric InAlAs/InGaAs/InP DGHEMT and the different device characteristics obtained were investigated. The distribution of carriers given by the density gradient model varies greatly from the distributions predicted by the standard drift-diffusion model (semi-classical model). To explore the applicability of the proposed quantum model to nanoscale DGHEMTs, observed simulation results were compared and found to agree well with the experimental results. Electron concentration profile shows significant deviations from semi-classical model. The wave functions extension into the barriers and also into the second quantum well modifies the electron distribution of the double triangular quantum well. The strong coupling between the two wells at nanodimensions causes them to behave like a single quantum well. Thus it is concluded that the quantization in the channel is very well explained by the proposed quantum model and should be incorporated to model the DGHEMT at nanodimensions.

ACKNOWLEDGMENT

The authors acknowledge University Grants Commission for providing financial support for this work.

REFERENCES

[1] L. Esaki and R. Tsu, "Superlattice and negative differential conductivity in semiconductors," *IBM J. Res. and Dev.,* Vol.14, No.1, pp.61-65, Jan., 1970.

[2] P. Ho, P. C. Chao, K. H. G. Duh, A. A. Jabra, J. M. Ballingall and P. M. Smith, "Extremely high gain, low noise InA1As/InGaAs HEMTs grown by MBE," *IEDM 1988, Technical Digest*, 11-14, pp. 184-186, Dec., 1988.

[3] U. K. Mishra, A. S. Brown, S. E. Rosenbaum, M. J. Delaney, S. Vaughn and K. White, "Noise performance of submicrometer AlInAs-GaInAs HEMTs," *IEEE Trans. on Electron Dev.*, Vol.35, No.12, pp.2441-2442, Dec., 1988.

[4] E. Sano, "InP HEMT lightwave communication ICs for 40 Gbit/s and beyond," *IPRM 1999, 11th IEEE International Conference on Indium Phosphide and Related Materials, 1999*, 16-20, pp.299-304, May, 1999.

[5] Y. Umeda, T. Enoki, T. Otsuji, T. Suemitsu, H. Yokoyama and Y. Ishii, "Ultrahigh-Speed IC technologies using InP based HEMTs for future optical communication systems," *IEICE Trans. on Electronics,* Vol.E82-C, No.3, pp.409-418, Mar., 1999.

[6] T. Enoki, H. Yokoyama, Y. Umeda and T. Otsuji,

"Ultra High speed integrated circuits using InP based HEMTs," *Jpn. J. Appl. Phys.*, Vol.37, No.3B, pp.1359-1364, Mar., 1998.

[7] Y. Kwon, D. Pavlidis, T. L. Brock and D. C. Streit, "Experimental and theoretical characteristics of high performance pseudomorphic double hetero-junction InAlAs/$In_{0.7}Ga_{0.3}As$/InAlAs HEMTs," *IEEE Trans. on Electron Dev.,* vol.42, No.6, pp.1017-1025, Jun., 1995.

[8] Y. Kwon, D. Pavlidis, T. L. Brock, G. I. Ng, K. L. Tan and J. R. Velebir, "Submicron pseudomorphic double heterojunction InAlAs/$In_{0.7}Ga_{0.3}As$/InAlAs HEMTs with high cut-off and current-drive capability," *IPRM 1993, 5th IEEE International Conference on Indium Phosphide and Related Materials, 1993*, 19-22, pp.465-468, Apr., 1993.

[9] N. Wichmann, I. Duszynski, S. Bollaert, J. Mateos, X. Wallart and A. Cappy, "100nm InAlAs/InGaAs Double-Gate HEMT using transferred substrate," *IEDM 2004, Technical Digest*, 13-15, pp. 1023-1026, Dec., 2004.

[10] B. G. Vasallo, N. Wichmann, S. Bollaert , A. Cappy, T. Gonzalez , D. Pardo and J. Mateos, "Monte Carlo Comparison Between InP-Based Double-Gate and Standard HEMTs," *EuMIC 2006*, *1st European Microwave Integrated Circuits Conference, 2006*, 10-13, pp.304-307, Sep., 2006.

[11] A-J Shey and W.H. Ku, "An analytical current–voltage characteristics model for high electron mobility transistors based on nonlinear charge-control formulation," *IEEE Trans. on Electron Dev*., Vol.36, No.10, pp.2299-2306, Oct., 1989.

[12] H. Brech, T. Grave, T. Simlinger and S. Selberherr, "Optimization of pseudomorphic HEMTs supported by numerical simulation," *IEEE Trans. on Electron Dev*., Vol.44, No.11, pp.1822-1828, Nov., 1997.

[13] H. Luth, "Nanostructures and Semiconductor Electronics," *phys. stat. sol.,* Vol.192, No.2, pp.287-299, Dec., 1995.

[14] E. Sano, "Simulation of Nanometer-scale Semiconductor Devices Considering Quantum Effects," *Int. J. RF. Microw CE*.,Vol.14, pp.283-289, Oct., 2004.

[15] G. Krokidis, J.P. Xanthakis, N.K. Uzunoglu, "A fully 2-dimensional, quantum mechanical calculation of short-channel and drain induced barrier lowering effects in HEMTs," *Solid-State Electron,* Vol.52, No.5, pp.625-631, May, 2008.

[16] ATLAS User's Manual, *Silvaco International*, 2010.

[17] C. L. Gardner and C. A. Ringhofer, "Smooth Quantum potential for the Hydrodynamic Model," *Phys. Rev. E.*, Vol.53, No.1, pp.157-167, Jan., 1996.

[18] A.Wettstein, *Quantum Effects in MOS Devices* (Hartung–Gorre Verlag Konstanz, 2000).

[19] A. Wettstein, A. Schenk, and W. Fichtner, "Quantum Device-Simulation with the Density Gradient Model on Unstructured Grids," *IEEE Trans. Electron Dev*., Vol.42, No.2, pp.279-283, Feb., 2001.

[20] A. Wettstein, O. Penzin and E. Lyumkis, "Integration of Density Gradient Model into a General Purpose Device Simulator," *VLSI Des*., Vol.15, No.4, pp.751-759, 2002.

[21] B. G. Vasallo, N. Wichmann, S. Bollaert, Y. Roelens, A. Cappy, T. Gonzalez, D. Pardo, and J. Mateos, "Comparison Between the Dynamic Performance of Double- and Single-Gate AlInAs/ InGaAs HEMTs," *IEEE Trans. on Electron Dev*., Vol.54, No.11, pp.2815-2822, Nov., 2007.

[22] J. R. Zhou and D. K. Ferry, "Simulation of ultra-small GaAs MESFET using quantum moment equations," *IEEE Trans. on Electron Dev*., Vol.39, No.3, pp.473-478, Mar., 1992.

[23] V. Mitin, V.A. Kochelap and M.A. Stroscio, "Quantum Heterostructures: Microelectronics and Optoelectronics," *Cambridge University Press, U.S.A*, 1999.

[24] N. Wichman, I. Duszynski, X. Wallart, S. Bollaert and A. Cappy, "InAlAs-InGaAs Double-Gate HEMTs on Transferred Substrate," *IEEE Electron Dev Lett.,* Vol.25, No.6, pp.354-356, Jun., 2004.

[25] D. Guerra, R. Akis, F. A. Marino, D. K. Ferry, S. M. Goodnick, M. Saraniti, "Aspect Ratio Impact on RF and DC Performance of State-of-the-Art Short-Channel GaN and InGaAs HEMTs," *IEEE Electron Dev Lett*., Vol.31, No.11, pp.1217-1219, Nov., 2010.

Neha Verma received the Bachelor of Applied Sciences, B.A.Sc. in Electronics (Honours) from University of Delhi, Delhi, India, in 2004 and M.Sc. in Electronics from Jamia Millia Islamia University, Delhi, India, in 2006. She is currently pursuing research at the Microelectronics Research Laboratory, Department of Electronic Science, A.R.S.D College, University of Delhi, South Campus, on Quantum Modeling and Simulation of double-gate InAlAs/InGaAs high electron mobility transistor.

Mridula Gupta received B.Sc. in Physics, M.Sc. in Electronics, M.Tech. in Microwave Electronics and Ph.D. in Optoelectronics from University of Delhi, Delhi, India, in 1984, 1986, 1988, and 1998, respectively. Since 1989, she has been with the Department of Electronic Science, University of Delhi South Campus, New Delhi, India, where she is currently a Professor and is also associated with Semiconductor Device Research Laboratory. She is the author/coauthor of approximately 235 publications in international and national journals and conference proceedings. She has supervised 14 Ph.D. students. She contributed the chapter entitled "MOSFET Modeling" in the *Encyclopedia on RF and Microwave Engineering* (Wiley, 2005). Her current research interests include modeling and simulation of MOSFETs, MESFETs and HEMTs for microwave-frequency applications.

R. S. Gupta received B.Sc. and M.Sc. degrees from Agra University, Agra, India, in 1963 and 1966, respectively, and Ph.D. degree in electronic engineering from the Institute of Technology, Banaras Hindu University, Varanasi, India, in 1970. In 1971, he was with Ramjas College, University of Delhi, Delhi, India. In 1987, he was with the Department of Electronic Science, University of Delhi South Campus, New Delhi, as a Reader and later as a Professor from 1997 to 2008. He was CSIR Emeritus Scientist with the Semiconductor Device Research Laboratory, Department of Electronic Science, University of Delhi, until March 2009. He heads several major research projects sponsored by the Ministry of Defense, the Department of Science and Technology, the Council of Science, and the Industrial Research and University Grants Commission. In 1988, he was a Visitor with the University of Sheffield, Sheffield, U.K., under the ALIS Link exchange program and also visited several U.S. and Spanish universities in 1995 and 1999, respectively. He also visited the Czech Republic in August 2003; Korea in November 2003; Rensselaer Polytechnic Institute, Troy, NY, in August 2004; and China in December 2005. In Dec 19, 2007 he visited Rome, Italy and in 2009 he visited North Texas University and Southeast Missouri State University USA. He contributed the chapter entitled "MOSFET Modeling" in the *Encyclopedia on RF and Microwave Engineering* (Wiley, 2005). His current interests and activities include modeling of SOI sub-micrometer MOSFETs and LDD MOSFETs, modeling and design of HEMTs, hot-carrier effects in MOSFETs, and modeling of GaAs MESFETs for high-performance microwave and millimeter-wave circuits and quantum-effect devices. Prof. Gupta was an Executive Member of the IEEE Electron Devices Society/Microwave Theory and Techniques Society Chapter of the IEEE India Council. Prof. Gupta is Life Senior Member IEEE and was Chairman of IEEE EDS Delhi Chapter. His name also appeared in the Golden List of the IEEE TRANSACTIONS ON ELECTRON DEVICES in December 1998, 2002, and 2004. He is a Fellow of the Institution of Electronics and Telecommunication Engineers (India), a Life Member of the Indian Chapter of the International Centre for Theoretical Physics, and a Life Member of the Semiconductor Society of India and chairman of society for microelectronics and VLSI. He was the Secretary of ISRAMT'93 and the 1996 Asia–Pacific Microwave Conference (APMC'96), and the Chairman of the Technical Programme Committee of APMC'96. He edited the proceedings of both of these international conferences. He was the Chairman of APMC'2004 held in New Delhi in December 2004. He has been listed in *Who's Who in the World*. Prof Gupta was chairman of 12^{TH} ISMOT 2009 held in Dec 2009 in India. He is the author/coauthor of over 600 papers in various

international and national journals and conference proceedings. 42 students have received their Ph.D. under his guidance. In addition to this he is currently supervising 8 students. He is currently a Professor and Head of the Department of Electronics & Communication Engineering, Maharaja Agrasen Institute of Technology (GGIP University, Delhi).

Jyotika Jogi received B.Sc. (Honours) in Physics, M.Sc. in Electronic Science, M.Phil. in Electronic Science, and Ph.D. in Microelectronics from the University of Delhi, Delhi, India, in 1986, 1988, 1990, and 2003, respectively. She was a Lecturer in Sri. Venkateswara College, University of Delhi, from 1988 to 1991 and has been teaching at the Atma Ram Sanatan Dharma College, University of Delhi, since 1991, as an Associate Professor in Electronic Science. Her main research interests are in the field of modeling and simulation of ultrahigh-speed devices and quantum heterostructures.